A sodium germanosilicide with unusual network topology

Julia-Maria Hübner[1*], Thomas B. Shiell[1], Piotr A. Guńka[2], Shuo Tao[3], Li Zhu[3], Mads Fonager Hansen[1], Emma S. Bullock[1], Stella Chariton[4], Vitali B. Prakapenka[4], Yingwei Fei[1], Vladislav A. Blatov[5], Davide M. Proserpio[6] and Timothy A. Strobel[1*]

[1]Earth and Planets Laboratory, Carnegie Institution for Science, Washington, District of Columbia 20015, United States

[2]Faculty of Chemistry, Warsaw University of Technology, 00-664 Warsaw, Poland

[3]Department of Physics, Rutgers University, Newark, NJ 07102, United States

[4]Center for Advanced Radiation Sources, The University of Chicago, Chicago, Illinois 60637, United States

[5]Samara Center for Theoretical Materials Science (SCTMS), Samara State Technical University, Samara 443100, Russia

[6]Dipartimento di Chimica, Università degli Studi di Milano, 20133 Milano, Italy

KEYWORDS: Intermetallics, framework compound, high pressure

ABSTRACT: The germanosilicide $Na_{4-x}Ge_ySi_{16-y}$ ($0.4 \le x \le 1.1$, $4.7 \le y \le 9.3$) was synthesized under high-pressure, high-temperature conditions. The novel guest–host compound comprises a unique tetrel framework with dual channels housing sodium and smaller, empty $(Si,Ge)_9$ units. The arrangement represents a new structure type with an overall structural topology that is closely related to a hypothetical carbon allotrope. Topological analysis of the structure revealed that the guest environment space cannot be tiled with singular polyhedra as in cage compounds (e.g., clathrates). The analysis of natural tilings provides a convenient method to unambiguously compare related tetrel-rich structures and can help elucidate new possible structural arrangements of intermetallic compounds.

Intermetallic compounds are typically ordered solids composed of two or more metals or semimetals, and the properties observed are often superior to the individual constituents.[1,2] For the case of silicon and germanium, a large number of binary intermetallic phases are known to exhibit large structural variety including simple close-packed arrangements, polyanionic Zintl phases, and more complex extended clathrate and open-framework networks hosting guest atoms.[3,4] This structural variety yields diverse physical properties that are important for a broad range of applications including catalysis,[5] solar-thermal applications,[6] thermoelectrics,[7,8] and superconductors.[9] While overarching principles that govern structural arrangements, stabilities, and physical properties are still being developed, the discovery of novel intermetallic compounds can facilitate a broader understanding of complex bonding interactions and open new possibilities for applications.[10,11]

High-pressure, high-temperature methods have proven to be versatile tools to access new compositions and structure types with exceptional properties.[12] Under compression, a volume reduction and, therefore, a densification of matter occurs, resulting in increased electrostatic interactions.[13] For the case of group-14 elements, a wide range of novel guest–host framework types and compositions have been synthesized under high-pressure conditions, in addition to the clathrate structures that are formed at low pressure.[14–29] Many framework types exhibit variable guest atom occupancies, and thus tunable electronic structures, and in some cases, guest atoms or intercalants may be topotactically removed to produce novel tetrel allotropes.[30–34] The exploration of higher-order systems with the possibility of multipartite frameworks adds additional degrees of freedom to expand the structural diversity of 3D frameworks.

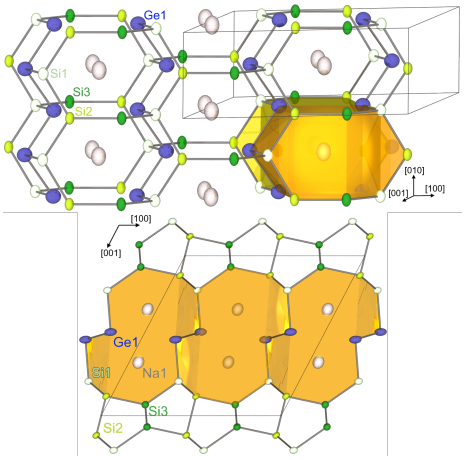

Figure 1. Crystal structure of $Na_{4-x}Ge_ySi_{16-y}$ with a network of (3*b*)Ge and (4*b*)Si/Ge forming dual channels (orange) housing two Na atoms and empty $(Si,Ge)_9$ units.

Herein, we report the synthesis of the novel compound $Na_{4-x}Ge_ySi_{16-y}$. The new structure comprises a 3D network of four- (4*b*) Si/Ge and three-bonded (3*b*) Ge atoms that incorporate Na into extended cavities (**Figure 1**). The Si:Ge ratio is tunable based on the starting composition. The cavities share similarities with other tetrel-rich compounds and a topological analysis of natural tilings allowed for the structural classification among the family of tetrelides.

The new compound, $Na_{4-x}Ge_ySi_{16-y}$ ($0.4(1) \le x \le 1.1(1)$, $5.5(2) \le y \le 9.9(2)$), was obtained by high-pressure, high-temperature synthesis (7.5 GPa, 500 ≤ *T* ≤ 650 °C for 1 to 3 h) from mixtures of the elements (synthesis procedure detailed in the **Supporting Information**). Recovered samples consist of grey pellets comprised of $Na_{4-x}Ge_ySi_{16-y}$ intergrown with Si/Ge alloy and an air-sensitive, sodium-rich phase (based on energy-dispersive X-ray spectroscopy, EDS, see **Table S9**). Crystals of the target phase can be isolated from crushed product agglomerates and persist after washing.

X-ray diffraction measurements reveal that $Na_{4-x}Ge_ySi_{16-y}$ crystallizes in space group *C*2/*m* with $a \approx 10.70$ Å, $b \approx 3.96$ Å, $c \approx 10.73$ Å and $\beta \approx 117.7°$ (**Table S1**). The final structural model was determined using single-crystal X-ray diffraction data (SXRD) obtained with synchrotron radiation (Advanced Photon Source, sector 13 ID-D). The refinement resulted in five atomic positions Na1, Si1, Si2, Si3, and Ge4. All Si positions exhibit mixed Si/Ge occupancy with the largest Ge fraction on Si1, in line with longer distances compared to contacts involving the Si2 and Si3 positions (**Table S6**, **S8**). No mixed Si/Ge occupancy was observed for Ge4, and the (3*b*)Ge–(3*b*)Ge distances (**Table S6**, **S8**) fall into the range of (3*b*)Ge–(3*b*)Ge distances in other alkali, alkaline earth, and rare earth germanides.[35] Na1 showed partial occupancy (the refinement procedure is detailed in the **SI**). The unit cell volumes refined from powder X-ray diffraction data (PXRD) increase with increasing Ge content in the precursor mixture (**Figure S1**, **Table S1**), indicating a larger amount of Ge substitution within the structure. The refined Ge:Si ratio for all samples varies between ~0.5–1.6 in agreement with EDS and wavelength-dispersive X-ray spectroscopy (WDS) (**Figures S1**, **S2**, **Tables S1-3**).

The structural arrangement consists of a 3D network of (3*b*)Ge and (4*b*)Si/Ge that form cassinoidal-shaped cavities housing two Na atoms (**Figure 1**). These cavities form extended channels along [010] that are alternatingly offset along [100]. In [001], one row of filled cavities is followed by puckered layers of hexagonal Si/Ge-rings forming empty $(Si,Ge)_9$ units. Interestingly, similar puckered layers and empty units are found in ternary P/Si and As/Si frameworks despite non-four-bonded pentel atoms.[36-38] The host lattice arrangement is closely related to a hypothetical 3D carbon allotrope that belongs to a class of topological nodal-line semimetals,[39] called *m*-C_8, reported in the carbon allotrope database SACADA as $3,4^3T71$.[40] The only difference between the frameworks is that three-center nodes (3*b*) of $Na_{4-x}Ge_ySi_{16-y}$ are pyramidal rather than flat as in the C allotrope.

The stacking arrangement of filled cavities in straight columns along [010] resembles stacking sequences in $MgSi_5$,[18] $LaSi_{10}$,[14] Na_4Ge_{13},[41] and MTt_6 (*M*=Na, Sr, Ba, Eu, *Tt*=Si, Ge).[16,19,42–44] Whereas (4*b*)Si/Ge^0 is the usual case for tetrel-based frameworks,[45] examples with (3*b*)Ge are known (see **Table S11**). Interestingly, three-bonded vertices are found in $BaGe_{6-x}$,[16] $SrGe_6$,[17] α-$LaSi_5$,[14] $LaGe_5$,[15] and $BaGe_5$[20] on opposing sides of filled cavities, as is observed in $Na_{4-x}Ge_ySi_{16-y}$. Seemingly, structures containing three-bonded species are associated with the occurrence of larger guest environments as compared with those comprised exclusively of four-bonded species.

To unambiguously classify the new germanosilicide among other 3D silicon- or germanium-based, guest–host frameworks, we performed a topological analysis of natural tiles[46] using ToposPro.[47] Whereas the crystal–chemical description of structural motifs relies on subjective interpretations,[48] the topological analysis utilizes a discrete set of rules to describe the tiling of 3D space.[46,49] Tetrel-rich (MTt_x, $x \ge 2$) alkali, alkaline earth, or rare earth metal compounds were compiled from the Inorganic Crystal Structure Database (ICSD)[50], resulting in 117 compounds with 20 different structure types total, and their structures were decomposed into natural tilings for topological analysis (**Figure 2**, **Table S11**).

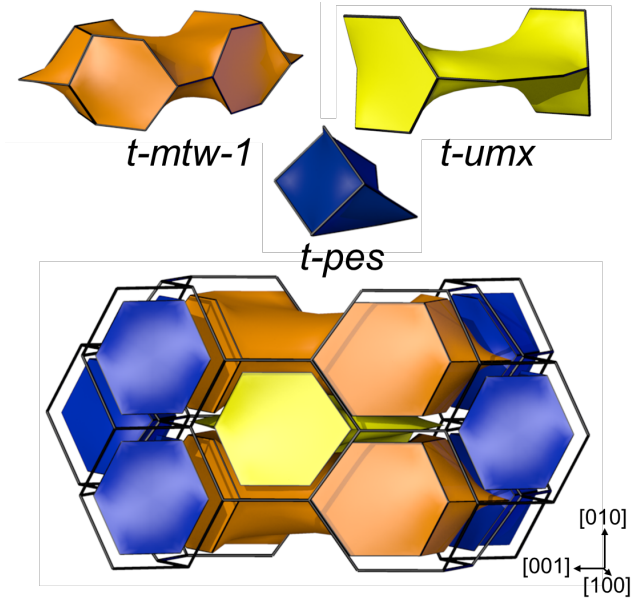

Figure 2. Framework tiling of $Na_{4-x}Ge_ySi_{16-y}$. The guest environment is represented by a combination of *t-mtw-1* and *t-umx* tiles.

The topological analysis revealed that the guest environments for these silicon- or germanium-rich frameworks can be either described by singular polyhedral tiles, or subdivided into multiple tile elements to fill 3D space (see **Table S11**). Single-tile polyhedral guest environments are defined as cages, as in clathrate compounds such as Na_8Si_{46}.[51] Other compounds, such as $MgSi_5$, $LaSi_{10}$, and type-VIII clathrates also contain single-tile guest environments, and therefore may be considered as cage-based compounds, but they also include additional non-guest-environment tiles. Another category of compounds investigated contains guest environments that are not unambiguously represented by one type of tiling. These types of guest environments are observed in several structures such as MTt_6 (*M*=Na, Sr, Ba, Eu, *Tt*=Si, Ge), and cannot be considered as cages due to their multi-tile nature. These types of structures are thus generally defined as open-framework compounds that contain cavities. Finally, several analyzed structures contain mixed motifs with both cage (single-tile) and cavity (multi-tile) guest environments. Cage-based structures exhibit the largest distances between guest atoms and generally have smaller maximum face ring sizes as compared with structures possessing non-cage (cavity) guest environments. The maximum ring sizes associated with the tiling elements for guest environments can serve as an additional measure for the classification of 3D networks as cage versus open-framework compounds (**Figure 3**).

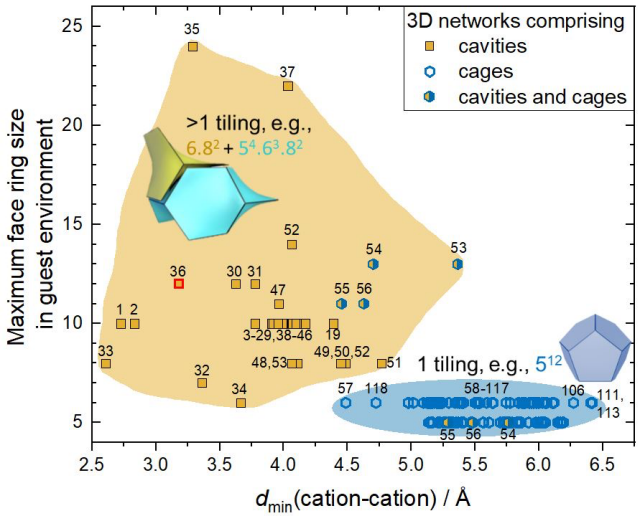

Figure 3. Minimum guest–guest distances vs. maximum face ring size (number of ring elements) for unique guest environments in tetrel-rich alkali, alkaline earth and rare earth metal silicides/germanides (see **Table S11**). $Na_{4-x}Ge_ySi_{16-y}$ is outlined in red.

The guest environments within $Na_{4-x}Ge_ySi_{16-y}$ cannot be represented by singular polyhedral tiles and consist instead of two tile types, *t–mtw–1* and *t–umx*, both found in zeolites (**Figure 2**, **Table S11**).[48] Therefore, $Na_{4-x}Ge_ySi_{16-y}$ is classified as an open-framework compound, which possesses cavities with shorter guest–guest distances and larger ring sizes compared to cage-based structures. The new compound also contains empty $(Si,Ge)_9$ units represented by *t-pes* tiles, as found in the zeolite EEI and the high-pressure compounds $NaSi_6$,[19] $SrGe_{6-x}$[52] and $SrGe_6$,[17] as well as *allo*-Si,[30] *allo*-Ge,[31,53-55] and $Li(Na)_7Ge_{12}$.[56] The novel framework is represented by a $3,4^3T71$ net according to the TopCryst system.[57] The underlying net can be related to hypothetical zeolites with *sqc*2060[58] (corresponding to Deem's[59] PCOD 8126237) and 4,4,4T3425-HZ[57] topology (Deem's PCOD 8045767), neither of which have been observed experimentally before. As the transformation to the first net comprises an intermediate 3D $3^2,4^2$-*c* net without change in space group, a solid-to-solid transformation becomes possible. Transformation to the latter topology requires an intermediate *honeycomb* net and, therefore, a decrease of net periodicity, pointing towards amorphization rather than structural transformation. Strikingly, no straightforward transformation pathway between the $3,4^3T71$ net and common 4-*c* tetrel nets exists, highlighting the unusualness of the new tetrel network (see **SI** for details). However, topologically similar networks are derived from slicing and rearranging diamond-type Si, highlighting the potential for further possible structural richness.[60]

Given the open-framework nature of $Na_{4-x}Ge_ySi_{16-y}$, Na mobility and guest atom removal are conceivable, similar to the formation of Si_{24} from $NaSi_6$[33] and predicted desodiation of Na_4Ge_4, $Na_{1-x}Ge_{3+z}$ and Na_xGe_{136}.[61] The theoretical storage capacity for the idealized stoichiometry $Na_4Ge_4Si_{12}$ was calculated based on Faraday's law to 149 $mAhg^{-1}$, which is similar to sodium battery materials such as $NaTiO_2$.[62] Despite the reduction of the Na content that was observed after samples were kept at ambient conditions for several weeks (**Figure S8- S10** and **Table S9**, **S10)** and upon heating to 100 °C (**Figure S4-S7**), the observed Na removal is accompanied by a broadening of PXRD reflections (**Figure S7, S10**) and an increase in the (Si,Ge) alloy content of the sample, indicating a degradation of the crystallites, and the 3D structure, as well as disproportionation (see **SI**).

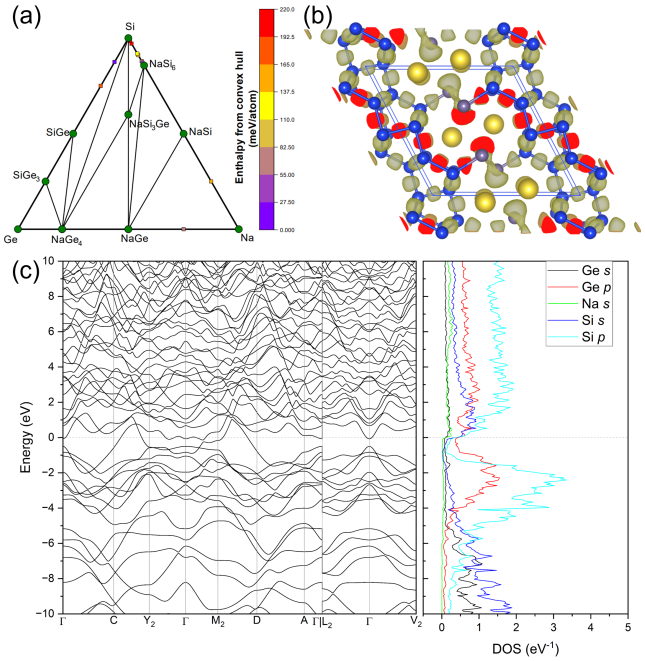

Figure 4. (a) Calculated Na–Si–Ge phase diagram at 10 GPa. Green circles indicate stable structures on the convex hull. Squares represent metastable structures colored by their hull distance. (b) ELF isosurface for $Na_4Ge_4Si_{12}$ where olive coloring represents ELF = 0.8. (c) Electronic band structure of $Na_4Ge_4Si_{12}$ with density of states (DOS) contributions projected onto atomic orbitals.

Density functional theory (DFT) calculations were performed on an idealized model $Na_4Ge_4Si_{12}$ without Ge substitution on (4*b*)-framework sites. At 10 GPa, this model structure is located on the ternary convex hull when considering known binary and ternary compounds in the Na–Si–Ge system (**Figure 4**), indicating that the new compound is likely thermodynamically stable under high-pressure conditions. At ambient pressure, $Na_4Ge_4Si_{12}$ remains dynamically stable with a formation enthalpy of ca. −153 meV/atom but is metastable with respect to known binaries (such as Na_4Ge_4 [63] and Na_8Ge_{46}/Na_xGe_{136}).[64]

According to the Zintl–Klemm concept, the occurrence of (3*b*)Ge and (4*b*)Si/Ge results in an electron balance of $Na^+_{4-x}[(3b)Ge^-]_y[(4b)Si^0]_{16-y}$. Nevertheless, the calculated band structure for the idealized composition $Na_4Ge_4Si_{12}$ shows metallic behavior with an appreciable density of states (DOS) at the Fermi level, pointing to a deviation from the idealized charge-balanced picture. The DOS plot shows significant contributions of the Ge *p* and Si *p* orbitals at the Fermi level, with Ge showing a more dominant role (**Figure 4**).

To understand this apparent contradiction, we probed the electronic structure through Electron Localization Function (ELF) and Bader charge analysis. Bader analysis revealed noticeable charge transfer from Na atoms to the Ge–Si framework. Notably, Ge atoms accumulate more charge than Si. This is consistent with the ELF results; the extra electrons of the 3*b* Ge form a lone pair, exhibiting sp^3 bonding characteristics. Additional crystal orbital Hamiltonian population (COHP) analysis provides detailed and atom-specific insights into the bonding nature of states within a particular energy window. For $Na_4Ge_4Si_{12}$, it is evident that a significant number of antibonding states are occupied below the Fermi level (**Figure S13**),

which is directly correlated with the occupied conduction bands and the metallic nature of the compound. This picture shows similarities to $SrGe_6$, which exhibits more complex guest–host bonding interactions compared with other open-framework compounds comprising cavities.[17] Given that the idealized $Na_4Ge_4Si_{12}$ stoichiometry was never observed experimentally, the complete picture involving partial Na occupancy and lattice substitutions is more complex.

In summary, a new type of Si/Ge framework was obtained by high-pressure, high-temperature techniques. The new guest–host compound $Na_{4-x}Ge_ySi_{16-y}$ ($0.4(1) \le x \le 1.1(1)$, $5.5(2) \le y \le 9.9(2)$) contains ellipsoidal cavities that house Na, while smaller empty $(Si,Ge)_9$ units complete the 3D space-filling arrangement. Topological analysis of natural tilings revealed a structural relationship with a hypothetical carbon allotrope and allowed for the classification among tetrel-rich silicides and germanides. The analysis revealed that guest environments comprising cages can be described by a single type of tiling, whereas open-framework structures require more than one type to describe one individual guest environment. Following the approach to predict new zeolite frameworks, the analysis of structural topology can be employed in the search for new intermetallic frameworks.

ASSOCIATED CONTENT

Supporting Information

The Supporting Information contains details about synthesis, meth-ods, as well as analyses results including powder and single crystal X-ray diffraction, X-ray spectroscopy, thermal analysis, crystal chemical and topological analysis and theoretical calculation details. The Supporting Information is available free of charge on the ACS Publications website.

AUTHOR INFORMATION

Corresponding Author

Julia-Maria Hübner - Earth and Planets Laboratory, Carnegie Institution for Science, Washington, District of Columbia 20015, United States
Email: jhubner@carnegiescience.edu and julia-maria.huebner@tu-dresden.de
Timothy A. Strobel - Earth and Planets Laboratory, Carnegie Institution for Science, Washington, District of Columbia 20015, United States
Email: tstrobel@carnegiescience.edu

Present Address

Julia-Maria Hübner – Faculty of Chemistry and Food Chemistry, Technische Universität Dresden, 01062 Dresden, Germany

ORCID

Julia-Maria Hübner: 0000-0003-2048-6629
Mads Fonager Hansen: 0000-0001-9006-4793
Emma S. Bullock: 0000-0002-5678-3695
Vitali B. Prakapenka :0000-0001-9270-2330
Stella Chariton: 0000-0001-5522-0498
Vladislav A. Blatov 0000-0002-4048-7218
Yingwei Fei: 0000-0001-9955-5353
Davide M Proserpio 0000-0001-6597-9406
Timothy A. Strobel: 0000-0003-0338-4380

Author Contributions

The manuscript was written through contributions of all authors. All authors have given approval to the final version of the manuscript.

Notes

The authors declare no competing financial interests.

ACKNOWLEDGMENT

This work was supported by the National Science Foundation, Division of Materials Research (NSF-DMR) by collaborative research awards 2226699 and 2226700. Portions of this work were performed at GeoSoilEnviroCARS (The University of Chicago, Sector 13), Advanced Photon Source (APS), Argonne National Laboratory. GeoSoilEnviroCARS is supported by the National Science Foundation–Earth Sciences (EAR-1634415). This research used resources of the Advanced Photon Source, a U.S. Department of Energy (DOE) Office of Science User Facility operated for the DOE Office of Science by Argonne National Laboratory under Contract No. DE-AC02-06CH11357. JMH gratefully acknowledges discussions about crystal structure refinements with Sven Lidin and Thomas Doert. DMP thanks the MUR for the grant PRIN2020 "Nature Inspired Crystal Engineering (NICE)".

REFERENCES

1. Westbrook, J. H. Intermetallic compounds: Their past and promise. *Metall. Trans. A* **1977**, 8, 1327–1360.
2. Gschneidner, K.; Russell, A.; Pecharsky, A.; Morris, J.; Zhang, Z.; Lograsso, T.; Hsu, D.; Lo, C. H. C.; Ye, Y.; Slager, A.; Kesse, D. A family of ductile intermetallic compounds. *Nature Mater.* **2003**, 2, 587–591.
3. Akhmetshina, T. G.; Blatov, V. A.; Proserpio, D. M.; Shevchenko, A. P. Topology of Intermetallic Structures: From Statistics to Rational Design. *Acc. Chem. Res.* **2018**, 51, 21–30.
4. Scharfe, S.; Kraus, F.; Stegmaier, S.; Schier, A.; Fässler, T. F. Zintl Ions, Cage Compounds, and Intermetalloid Clusters of Group 14 and Group 15 Elements. *Angew. Chem. Int. Ed.* **2011**, 50 (16), 3630–3670.
5. Furukawa, S.; Komatsu, T. Intermetallic Compounds: Promising Inorganic Materials for Well-Structured and Electronically Modified Reaction Environments for Efficient Catalysis. *ACS Catal.* **2017**, 7 (1), 735–765.
6. Gokon, N.; Jie, C. S.; Nakano, Y.; Okazaki, S.; Kodama, T.; Hatamachi, T.; Bellan, S. Phase Change Material of Copper–Germanium Alloy as Solar Latent Heat Storage at High Temperatures. *Front. Energy Res.* **2021**, 9, 696213.
7. Mori, T.; Vaney, J.; Guélou, G.; Failamani, F.; Guo, Q. Crystal growth of intermetallic thermoelectric materials. In: *Crystal Growth of Intermetallics*. Gille, P., Grin, Yu., Eds.; De Gruyter, **2019**, 217-260.
8. Cohn, J. L.; Nolas, G. S.; Fessatidis, V.; Metcalf, T. H.; Slack, G. A. Glasslike Heat Conduction in High-Mobility Crystalline Semiconductors. *Phys. Rev. Lett.* **1999**, 82, 779–782.
9. Kawaji, H.; Horie, H.; Yamanaka, S.; Ishikawa, M. Superconductivity in the Silicon Clathrate Compound $(Na,Ba)_xSi_{46}$. *Phys. Rev. Lett.* **1995**, 74, 1427– 1429.
10. Lin, Q.; Miller, G. J. Electron-Poor Polar Intermetallics: Complex Structures, Novel Clusters, and Intriguing Bonding with Pronounced Electron Delocalization. *Acc. Chem. Res.* **2018**, 51 (1), 49–58.

11. Nesper, R. Bonding Patterns in Intermetallic Compounds *Angew. Chem. Int. Ed*. **1991**, 30 (7), 789-817.
12. Walsh, J. P. S.; Freedman, D. E. High-Pressure Synthesis: A New Frontier in the Search for Next-Generation Intermetallic Compounds. *Acc. Chem. Res*. **2018**, 51 (6), 1315–1323.
13. Demazeau, G.; Huppertz, H.; Alonso, J. A.; Pöttgen, R.; Moran, E.; Attfield, J. P. Materials Chemistry under High Pressures - Some Recent Aspects. *Z. Naturforsch*., **2006**, 61b, 1457–1470.
14. Yamanaka, S.; Izumi, S.; Maekawa, S.; Umemoto, K. Phase diagram of the La-Si binary system under high pressure and the structures of superconducting $LaSi_5$ and $LaSi_{10}$. *J. Solid State Chem*. **2009**, 182 (8), 1991-2003.
15. Fukuoka, H.; Yamanaka, S. High-pressure synthesis and superconductivity of $LaGe_5$ containing a tunnel germanium network. *Phys. Rev. B*. **2003**, 67 (9), 094501-1-5.
16. Akselrud, L.; Wosylus, A.; Castillo, R.; Aydemir, U.; Prots, Y.; Schnelle, W.; Grin, Y.; Schwarz, U. $BaGe_6$ and $BaGe_{6-x}$: incommensurately ordered vacancies as electron traps. *Inorg. Chem*. **2014**, 53 (24), 12699-12705.
17. Schwarz, U.; Castillo, R.; Hübner, J. M.; Wosylus, A.; Prots, Y.; Bobnar, M.; Grin, Y. The untypical high-pressure Zintl phase $SrGe_6$. *Z. Naturforsch. B* **2020**, 75 (1-2), 209-216.
18. Hübner, J.-M.; Carrillo-Cabrera, W.; Prots, Yu.; Bobnar, M.; Schwarz, U.; Grin, Yu. Unconventional Metal-Framework Interactions in $MgSi_5$. *Angew. Chem. Int. Ed*. **2019**, 58 (37), 12914-12918.
19. Kurakevych, O. O.; Strobel, T. A.; Kim, D. Y.; Muramatsu, T.; Struzhkin, V. V. Na-Si clathrates are high-pressure phases: A melt-based route to control stoichiometry and properties. *Cryst. Growth Des*. **2013**, 13 (1) 303-307.
20. Aydemir, U.; Akselrud, L.; Carrillo-Cabrera, W.; Candolfi, C.; Oeschler, N.; Baitinger, M.; Steglich, F.; Grin, Yu. $BaGe_5$: A new type of intermetallic clathrate. *J. Am. Chem. Soc*. **2010**, 132 (32), 10984-10985.
21. Cros, C.; Pouchard, M.; Hagenmuller, P. Sur deux nouvelles structures du silicium et du germanium de type Clathrate. *Bull. Soc. chim. Fr.* **1971**, 379-386.
22. Castillo, R.; Carrillo-Cabrera, W.; Schwarz, U.; Grin, Yu. Classical and Nonclassical Germanium Environments in High-Pressure $BaGe_5$. *Inorg. Chem*. **2015**, 54 (3), 1019-1025.
23. Hübner, J.-M.; Carrillo-Cabrera, W.; Koželj, P.; Prots, Yu.; Baitinger, M.; Schwarz, U.; Jung, W. A Borosilicide with Clathrate VIII Structure, *J. Am. Chem Soc*. **2022**, 144 (30), 13456–13460.
24. Fukuoka, H.; Ueno, K., Yamanaka, S. High-pressure synthesis and structure of a new silicon clathrate $Ba_{24}Si_{100}$. *J. Organomet. Chem*. **2000**, 611 (1-2), 543-546.
25. Fukuoka, H.; Kiyoto, J.; Yamanaka, S. Superconductivity of metal deficient silicon clathrate compounds $Ba_{8-x}Si_{46}$ ($0 < x < 1.4$). *Inorg. Chem*. **2003**, 42, 2933-2937.
26. Yamanaka, S.; Komatsu, M.; Tanaka, M.; Sawa, H.; Inumaru, K. High-pressure synthesis and structural characterization of the type II clathrate compound $Na_{30.5}Si_{136}$ encapsulating two sodium atoms in the same silicon polyhedral cages. *J. Am. Chem. Soc*. **2014**, 136 (21), 7717-7725.
27. Gunatilleke, W.D.C.B.; Ojo, O.P.; Poddig, H.; Nolas, G.S. Synthesis and characterization of phase-pure clathrate-II $Rb_{12.9}Si_{136}$. *J. Solid State Chem*. **2022**, 311, 123-152.
28. Guloy, A. M.; Tang, Z.; Ramlau, R.; Böhme, B.; Baitinger, M.; Grin, Yu. Synthesis of the clathrate-II $K_{8.6(4)}Ge_{136}$ by oxidation of K_4Ge_9 in an ionic liquid. *Eur. J. Inorg. Chem*. **2009**, 17, 2455-2458.
29. Wosylus, A.; Veremchuk, I.; Schnelle, W.; Baitinger, M.; Schwarz, U.; Grin, Yu. $Cs_{8-x}Si_{46}$: A type-I clathrate with expanded silicon framework. *Chem. Eur. J.* **2009**, 15 (24), 5901-5903.
30. von Schnering, H.G.; Schwarz, M.; Nesper, R. The Lithium Sodium Silicide Li_3NaSi_6 and the formation of Allo-Silicon. *J. Less Common Met.* **1988**, 137, 297-310.
31. Kiefer, F.; Karttunen, A. J.; Döblinger, M.; Fässler, T. F. Bulk Synthesis and Structure of a Microcrystalline Allotrope of Germanium (*m-allo*-Ge). *Chem. Mater*. **2011**, 23, 4578–4586.
32. Gryko, J.; McMillan, P. F.; Marzke, R. F.; Ramachandran, G. K.; Patton, D.; Deb, S. K.; Sankey, O. F. Low-density framework form of crystalline silicon with a wide optical band gap. *Phys. Rev. B* **2000**, 62, R7707(R).
33. Kim, D. Y.; Stefanoski, S.; Kurakevych, O. O.; Strobel, T. A. Synthesis of an open-framework allotrope of silicon. *Nature Mat.* **2015**, 14 (2),169-173.
34. Guloy, A. M.; Ramlau, R.; Tang, Z.; Schnelle, W.; Baitinger, M.; Grin, Y. A guest-free germanium clathrate. *Nature* **2006**, 443, 320-323.
35. Freccero, R.; Frick, E.; Wilthorn, C.; Hübner, J.-M. New Insights into the Crystal Chemistry of FeB-Type Compounds: The Case of CeGe. *Materials* **2022**, 15, 9089.
36. Eisenmann, B.; Jordan, H.; Schäfer, H. $Ba_3Si_4P_6$, eine neue Zintlphase mit vernetzten Si_4P_5-Käfigen. *Z. Naturforsch. B* **1984**, 39, 864-867.
37. Toffoletti, L.; Kirchhain, H.; Landesfeind, J.; Klein, W.; van Wuellen, L.; Gasteiger, H. A.; Fässler, T. F. Lithium ion mobility in lithium phosphidosilicates: Crystal structure, ^{7}Li, ^{29}Si, and ^{31}P MAS NMR spectroscopy, and impedance spectroscopy of Li_8SiP_4 and Li_2SiP_2. *Chem. Eur. J*. **2016**, 22 (49), 17635-17645.
38. Haffner, A.; Weippert, V.; Johrendt, D. The phosphidosilicates $SrSi_7P_{10}$ and $BaSi_7P_{10}$. *Z. Anorg. Allg. Chem*. **2021**, 647 (4), 326-330.
39. Sung, H.-J.; Kim, S.; Lee, I.-H.; Chang, K.J. Semimetallic carbon allotrope with a topological nodal line in mixed sp^2-sp^3 bonding networks. *NPG Asia Materials*, **2017**, 9, e361.
40. Hoffmann, R.; Kabanov, A. A.; Golov, A. A.; Proserpio, D. M. Homo Citans and Carbon Allotropes: For an Ethics of Citation. *Angew. Chem. Int. Ed*. **2016**, 55, 10962–10976.
41. Stefanoski, S.; Finkelstein, G. J.; Ward, M. D.; Zeng, T.; Wei, K.; Bullock, E. S.; Beavers, C. M.; Liu, H.; Nolas, G. S.; Strobel, T. A. Zintl ions within framework channels. The complex structure and low-temperature transport properties of Na_4Ge_{13}. *Inorg. Chem*. **2018**, 57 (4), 2002-2012.
42. Wosylus, A.; Prots, Yu.; Burkhardt, U.; Schnelle, W.; Schwarz, U.; Grin, Yu. High-pressure synthesis of strontium hexasilicide. *Z. Naturforsch., B* **2006**, 61 (12), 1485-1492.
43. Yamanaka, S.; Maekawa, S. Structural evolution of the binary system Ba-Si under high-pressure and high-temperature conditions. *Z. Naturforsch. B* **2006**, 61 (12), 1493-1499.
44. Wosylus, A.; Prots, Yu.; Burkhardt, U.; Schnelle, W.; Schwarz, U.; Grin, Yu. Breaking the Zintl rule: high-pressure synthesis of binary $EuSi_6$ and its ternary derivative $EuSi_{6-x}Ga_x$ ($0 =< x =< 0.6$). *Solid State Sci*. **2006**, 8 (7), 773-781.
45. Hübner, J.-M. Beiträge zu Verbindungen von Silicium und Germanium mit Erdalkali-und Seltenerdmetallen unter Druck. *Dissertation, TU Dresden*, **2021**.
46. Blatov, V. A.; Delgado-Friedrichs, O.; O'Keeffe, M.; Proserpio, D. M. Three-periodic nets and tilings: natural tilings for nets. *Acta Crystallogr., Sect. A: Found. Crystallogr.* **2007**, A63, 418–425.
47. Blatov, V. A.; Shevchenko, A. P.; Proserpio, D. M. Applied Topological Analysis of Crystal Structures with the Program Package ToposPro. *Cryst. Growth Des*. **2014**, 14 (7), 3576–3586.

48. Blatova, O. A.; Golov, A. A.; Blatov, V. A. Natural tilings and free space in zeolites: models, statistics, correlations, prediction. *Z. Kristallogr*. **2019**, 234 (7–8), 421–436.
49. Blatov, V. A.; Ilyushin, G. D.; Proserpio, D. M. The zeolite conundrum: why are there so many hypothetical zeolites and so few observed? A possible answer from the zeolite-type frameworks perceived as packings of tiles. *Chem. Mater.* **2013**, 25, 412-424.
50. Zagorac, D.; Müller, H.; Ruehl, S.; Zagorac, J.; Rehme, S. Recent developments in the Inorganic Crystal Structure Database: theoretical crystal structure data and related features. *J. Appl. Cryst*. **2019**, 52, 918-925.
51. Dolyniuk, J.A.; Owens-Baird, B.; Wang, J.; Zaikina, J. V.; Kovnir, K. Clathrate thermoelectrics. *Mater. Sci. Eng. R* **2016**, 108, 1-46.
52. Fukuoka, H.; Yamanaka, S.; Matsuoka, E. Takabatake, T. High-Pressure Synthesis and Transport Properties of a New Binary Germanide, $SrGe_{6-\delta}$ ($\delta \cong 0.5$), with a Cagelike Structure. *Inorg. Chem*. **2005**, 44 (5), 1460–1465.
53. Grüttner, A.; Nesper, R.; von Schnering, H.G. Novel Metastable Germanium Modifications *allo*-Ge and 4*H*-Ge from Li_7Ge_{12}. *Angew. Chem. Int. Ed*., **1982**, 21, 912-913.
54. Conesa, J. C, Computer Modeling of allo-Si and allo-Ge Polymorphs. *J. Phys. Chem. B* **2002**, 106 (13), 3402-3409.
55. Tang, Z.; Litvinchuk, A. P.; Gooch, M.; Guloy, A. M. Narrow Gap Semiconducting Germanium Allotrope from the Oxidation of a Layered Zintl Phase in Ionic Liquids. *J. Am. Chem. Soc*. **2018**, 140 (22), 6785-6788.
56. Grüttner, A.; Nesper, R.; von Schnering, H. G. New Phases in the Li-Ge System: Li_7Ge_{12}, $Li_{12}Ge_7$, and $Li_{14}Ge_6$. *Acta Crystallogr., Sect. A: Cryst. Phys., Diffr., Theor. Gen. Cryst.* **1981**, 37, C161.
57. Shevchenko, A. P.; Shabalin, A. A.; Karpukhin, I. Y.; Blatov, V. A. Topological Representations of Crystal Structures: Generation, Analysis and Implementation in the TopCryst System. *Sci. Technol. Adv. Mater. Methods* **2022**, 2 (1), 250–265.
58. Ramsden, S. J.; Robins, V.; Hyde, S. T. Three-dimensional Euclidean nets from two-dimensional hyperbolic tilings: kaleidoscopic examples. *Acta Crystallogr Sect A*. **2009**, 65 (2), 81–108.
59. Pophale, R.; Cheeseman, P. A.; Deem, M. W. A Database of New Zeolite-Like Materials. *Phys. Chem. Chem. Phys*. **2011**, 13, 12407-12412.
60. Jantke, L. A.; Stegmaier, S.; Karttunen, A. J.; Fässler, T. F. Slicing Diamond—A Guide to Deriving sp^3-Si Allotropes. *Chem. Eur. J*. **2017**, 23 (12), 2734-2747.
61. Nandakumar, A.; Peng, X.; Chan, C. K. Type II Germanium Clathrates from Zintl Phase Precursor Na_4Ge_4: Understanding Desodiation Processes and Sodium Migration Using First-Principles Calculations. *J. Phys. Chem. C* **2023**, 127 (27), 12882–12894.
62. Wu, D.; Li, X.; Xu, B.; Twu, N.; Liu, L.; Ceder, G. $NaTiO_2$: a layered anode material for sodium-ion batteries. *Energy Environ. Sci.* **2015**, 8, 195-202.
63. Witte, J.; von Schnering, H. G.; Hagenmuller, P. Die Kristallstruktur von NaSi und NaGe. *Z. Anorg. Allg. Chem*. **1964**, 327, 260-273.
64. Horie, H.; Kikudome, T.; Teramura, K.; Yamanaka, S. Controlled thermal decomposition of NaSi to derive silicon clathrate compounds. *J. Solid State Compds*. **2009**, 182 (1), 129-135.